

Anisotropic magnetoresistance in atomic chains of iridium and platinum from first principles

Víctor M. García-Suárez,¹ David Zs. Manrique,^{1,2} Colin J. Lambert,¹ and Jaime Ferrer^{2,*}

¹*Department of Physics, Lancaster University, Lancaster LA1 4YB, United Kingdom*

²*Departamento de Física, Universidad de Oviedo, 33007 Oviedo, Spain*

(Received 7 October 2008; revised manuscript received 17 December 2008; published 18 February 2009)

We analyze the magnetoresistance ratio of finite and infinite iridium and platinum chains. Our calculations, which are based on a combination of the nonequilibrium Green's function techniques and density-functional theory, include a fully self-consistent treatment of noncollinear magnetism and of the spin-orbit interaction. They indicate that, in addition to having an extremely large magnetic anisotropy, infinite and also realistic finite-length iridium chains show sizeable anisotropic magnetoresistance ratios. We therefore propose iridium nanostructures as promising candidates for nanospintronics logic devices.

DOI: 10.1103/PhysRevB.79.060408

PACS number(s): 75.30.Gw, 75.47.-m, 85.75.-d, 73.43.Qt

The ability to enhance and tailor the magnetic anisotropy and magnetoresistance of atomic-sized magnetic bits and junctions will determine whether nanospintronics will be a viable technology. Cobalt clusters and chains with magnetic anisotropy energy (MAE) barriers of the order of 1 meV were fabricated a few years ago by their deposition on substrates of *5d* elements.^{1,2} Furthermore, several recent theoretical predictions have pointed out that atomic clusters and chains made of *4d* elements should have even higher magnetic anisotropy barriers than Co nanostructures.³⁻⁵ In the case of *5d* elements such as platinum and iridium, calculations predict that the anisotropies of iridium and platinum atomic clusters and chains can be even larger than room-temperature thermal energies so that these nanostructures can overcome the technologically relevant superparamagnetic limit.^{4,6,7}

Suspended chains of gold atoms that connected two gold electrodes were fabricated using the scanning tunneling microscope and mechanically controllable break junction (MCBJ) techniques,^{8,9} where a quantized conductance close to $G_0=2e^2/h$ was measured. Subsequent experiments found that platinum and iridium also formed suspended chains but that other elements such as Ni, Co, Pd, or Rh did not,^{10,11} unless doped with oxygen or other elements.¹² It was also demonstrated that longer atomic chains could be made by deposition on stepped surfaces¹ or by encapsulation in carbon nanotubes.¹³

The reduced dimensionality of nanometric objects increases their tendency toward magnetism. Ugarte and co-workers¹⁴ proposed that their experimental conductance data for platinum chains could be explained provided that these were magnetic. Subsequent theoretical work indeed found that *4d* and *5d* infinite linear chains of bulk-paramagnetic materials do become magnetic.^{15,16} Very recently, several groups have found that the MAE per atom of infinite zigzag platinum and iridium chains⁶ and of linear platinum chains⁷ show values as large as 50–100 meV when stretched. We draw attention in this Rapid Communication to iridium and platinum atomic structures as promising candidates for nanospintronics. We show that iridium atomic chains not only have huge magnetic anisotropies but also meet the requirement of having a significant magnetoresistance ratio. The simulations presented here are based on density-functional theory¹⁷ as implemented in the SIESTA code¹⁸ and include a fully self-consistent implementation of

the spin-orbit interaction.^{19,20} This spin-orbit implementation has been successfully used to compute the magnetic anisotropy of infinite Ir and Pt atomic chains⁶ and of transition-metal atomic clusters,⁴ in agreement with the results of other simulations.^{3,5,7} The conductance calculations were carried out with our code SMEAGOL,²¹ which includes the fully self-consistent implementation of the spin-orbit interaction referred to above. We note that SMEAGOL has been shown to provide conductance data that compare rather accurately with the available experimental data on platinum chains.^{10,11,22} The simulations have used the local-density

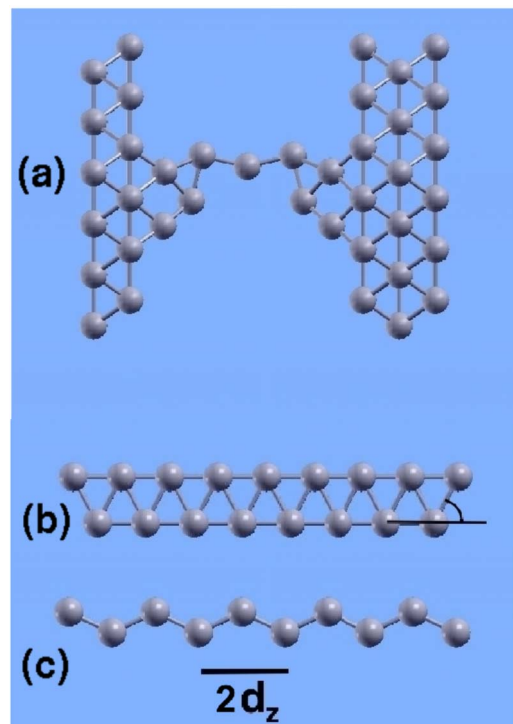


FIG. 1. (Color online) The geometry of the chains simulated in this Rapid Communication referred to the three coordinate axes. (a) Schematic view of the geometry of the relaxed finite-length chains in contact to two electrodes; (b) ladder geometry that corresponds to the absolute minimum of the infinite chains, see the top-right panel in Figs. 2 and 3; (c) zigzag geometry that corresponds to the second minimum of the infinite chains, see the top-right panels in Figs. 2 and 3.

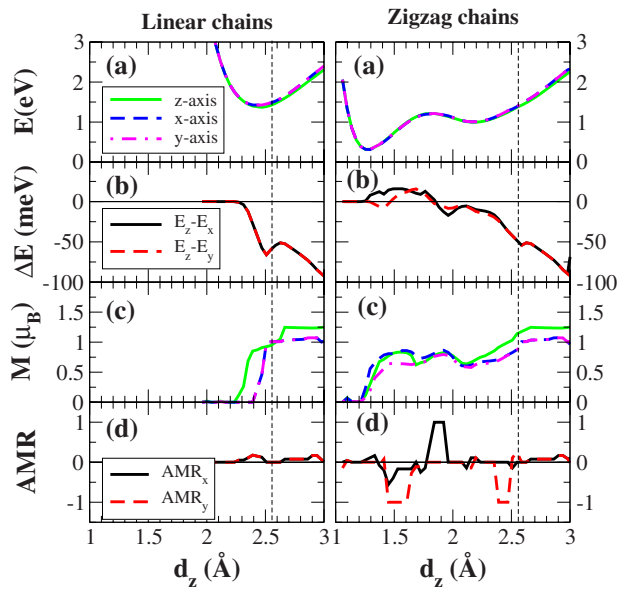


FIG. 2. (Color online) Results of the simulations of infinite platinum chains as a function of the distance d_z defined in Fig. 1 for orientations of the spins along the x , y , and z axes. The left panels correspond to the case of metastable linear chains. The right panels correspond to the geometries (b) and (c) in Fig. 1. The dashed vertical line indicates the distance d_z at which the zigzag chains cease to be stable. (a) Energies $E_{x,y,z}$ per atom; (b) magnetic anisotropy energies per atom $\Delta_{x,y}$; (c) spin moments per atom; (d) magnetoresistance ratio.

approximation²³ and norm-conserving pseudopotentials.²⁴ The atomic parameters that were fed in the pseudopotential generator, as well as the basis set used, are similar to those reported in Refs. 4, 6, and 22. They shed lattice constants of 3.82 and 3.92 Å for fcc iridium and platinum, whereas the experimental values are 3.84 and 3.92 Å, respectively.

Figure 1(a) shows a schematic view of the experimental setup of a MCBJ experiment, where at the last stages before breakage of a Pt or Ir strip, a short suspended atomic chain is formed. In these experiments, an electric current is applied to the circuit, and the conductance G is measured many times as the chain elongates. The whole setup can also be understood as a magnetic junction that connects two paramagnetic electrodes. Recent work has shown that theory can reproduce accurately the experimental conductance data of finite-length platinum chains²² but has not found significant differences between the paramagnetic and the magnetic cases.²⁵

We show the energy of linear platinum and iridium chains as a function of d_z in the left panels of Figs. 2(a) and 3(a). It is important to notice that these chains are metastable. Indeed, allowing for lateral displacements of the atoms yields the energy curves in the right panels of Figs. 2(a) and 3(a), which only have minima for ladder or zigzag arrangements similar to those shown in Figs. 1(b) and 1(c). Furthermore, relaxation of the forces always finishes in zigzag or ladder chains, unless the atoms are constrained to lie in a linear array. Actually, ladders are energetically more stable than zigzag geometries. But the relaxation of the forces in a MCBJ geometry, such as the one shown in Fig. 1(a), only leads to zigzag arrangements that gradually straighten as the

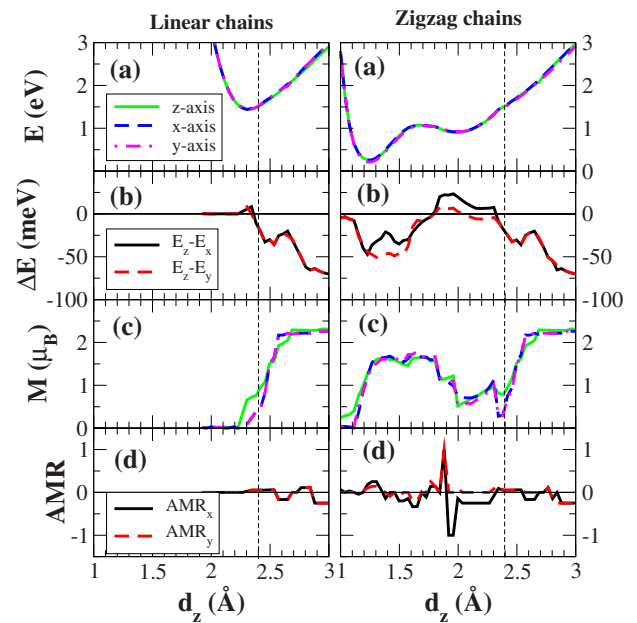


FIG. 3. (Color online) Results of the simulations of infinite iridium chains as a function of the distance d_z defined in Fig. 1 for orientations of the spins along the x , y , and z axes. The left panels correspond to the case of metastable linear chains. The right panels correspond to the geometries (b) and (c) in Fig. 1. The dashed vertical line indicates the distance d_z at which the zigzag chains cease to be stable. (a) Energies $E_{x,y,z}$ per atom; (b) magnetic anisotropy energies per atom $\Delta_{x,y}$; (c) spin moments per atom; (d) magnetoresistance ratio.

electrodes are pulled apart. Related to this effect, we note that infinite platinum (iridium) zigzag chains become linear only for distances d_z longer than 2.55 Å (2.40 Å) since at these distances, the zigzag angles fall abruptly to zero.⁶ These values of d_z are marked by a dotted vertical line in the right panels of Figs. 2 and 3. We will present results for the conductance of infinite zigzag and linear, as well as finite zigzag, chains in this Rapid Communication.

We have performed separate simulations for orientations of the atomic spins along the chain axis (z axis), perpendicular to it but still in the zigzag plane (x axis) and perpendicular to the zigzag plane (y axis), but the energies $E_{x,y,z}$ cannot be discriminated in the energy scale used in Figs. 2(a) and 3(a). We have therefore computed⁶ the energy differences $\Delta_{x,y} = E_z - E_{x,y}$ per atom, which we define as the MAEs, and plotted them in Figs. 2(b) and 3(b) for platinum and iridium, respectively. Our definition implies that when both $\Delta_{x,y}$ are negative, the magnetization lies parallel to the chain axis. On the contrary, when $\Delta_{x,y}$ is positive, the magnetization is oriented perpendicular to the chain axis and is aligned either parallel to the x or the y axis, depending on whether Δ_x is larger or smaller than Δ_y , respectively. Notice that our results for linear platinum chains [left panel in Fig. 2(b)] are similar to those presented in Ref. 7. More interestingly, the anisotropy of zigzag platinum and iridium chains is the x axis for short d_z but shifts to chain axis if the chains are elongated, with the MAE achieving values as large as 50–80 meV depending on the specific value of d_z . The third row in Figs. 2 and 3 shows the spin moment per atom as a function of d_z .

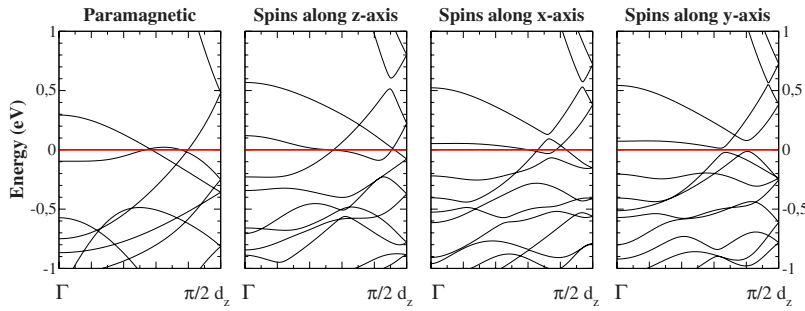


FIG. 4. (Color online) Band structure of a zigzag platinum chain with an elongation $d_z = 2.45 \text{ \AA}$. From left to right the panels show the bands for a paramagnetic calculation and for spin-orbit simulations, whereby the spins are oriented along the z , x , and y axes, respectively.

Smogunov *et al.*⁷ found that linear platinum chains become magnetized at a shorter elongation d_z for spin lying in the axis of the chain than for spins oriented perpendicular to it. This fact led them to predict a colossal magnetic anisotropy for the window of elongations within the onset of both magnetizations. However, we note here that the magnetization of the more realistic zigzag chains is nonzero for almost the full range of elongations regardless of the spin orientation, and therefore that effect is not expected to be seen. Interestingly, we find that the magnetization of iridium chains decreases when the chains are pulled apart in a window of elongations around the equilibrium d_z .

Since infinite Ir and Pt chains show large MAEs, an obvious question is whether they also show a strong anisotropic magnetoresistance (AMR) effect that can be activated by the presence of a magnetic field. If so, this effect could open the way toward room-temperature inorganic nanomagnetic memory bits. We have computed the low-voltage conductance $G_{x,y,z}$ for orientations of the spins along the three axes, which we have used to estimate the magnetoresistance ratio

$$\text{AMR}_{x,y} = \frac{G_{x,y} - G_z}{G_{x,y} + G_z}. \quad (1)$$

We note that if all the conductances are equal, then $\text{AMR}_{x,y}$ is zero. On the contrary, if one or two of the conductances fall to zero, then one or two of the ratios reach ± 1 , which we take as the signature of a perfect anisotropic magnetoresistance effect. $\text{AMR}_{x,y}$ for iridium and platinum chains is plotted as a function of d_z in Figs. 2(d) and 3(d), respectively. We find that the AMR ratio of linear chains is quite small, while zigzag chains on the contrary show sizeable ratios, which even reach ± 1 for some ranges of elongations, around the equilibrium distance.

More specifically, AMR_y in platinum chains shows a window of perfect magnetoresistance for elongations just above

the equilibrium distance. Further, the magnetization lies along the chain axis for these elongations. The range of d_z showing perfect magnetoresistance lies just below the equilibrium distance in iridium chains. On the positive side, the ratio AMR_x is nonzero for a longer range of elongations than in platinum chains. Notice that the anisotropy forces the magnetization to point along the x axis in that same d_z range.

Since the above nonzero magnetoresistance ratios originate from the different number of channels available for electron conduction close to the Fermi energy for the different spin orientations, we now study the band structure of infinite chains. Indeed, the number of conduction channels can be found by counting the number of bands crossing the Fermi energy. We note that each band moves up or down in energy at a different pace as the chain elongates. Furthermore, since the spin-orbit interaction couples spin and orbital degrees of freedom, these shifts are different for the different spin orientations. Since the band structure of nonconducting chains must show a minigap at the Fermi energy, we have plotted in Fig. 4 the band structure of a platinum chain at $d_z = 2.45 \text{ \AA}$ for paramagnetic as well as for spin-orbit simulations. We indeed find that when the atomic spins point in the y axis there exists a small minigap $E_g = 25 \text{ meV}$ at $k = 0.4\pi/d_z$. This value allows us to estimate the minimum number of atoms N that a finite-sized platinum chain must have to develop such minigaps. Using the relationship $N \approx \hbar v_F / E_g d_z$, where we estimate the Fermi velocity at this k point as $\hbar v_F \approx 1000 \text{ meV d}_z$, we find a critical length of about 40 atoms. We therefore expect that it will be difficult to measure a significant magnetoresistance ratio in platinum chains. We have indeed simulated five-atom-long platinum chains contacted to (001) platinum electrodes in a geometry similar to Fig. 1(a) and found that the magnetoresistance ratio was essentially zero.

In contrast, Fig. 5 shows the band structures of iridium chains obtained from paramagnetic and also for spin-orbit simulations for an elongation d_z such that G_x falls to zero.

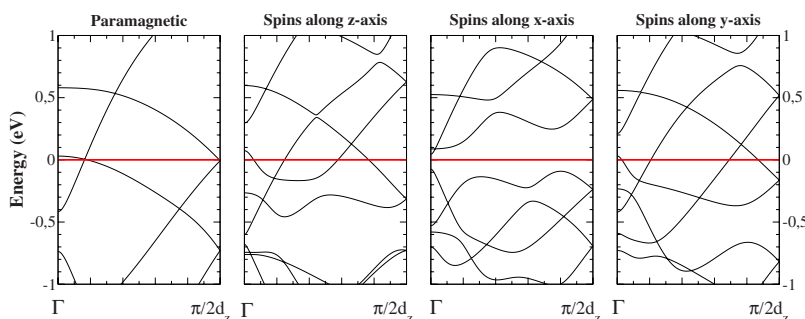


FIG. 5. (Color online) Band structure of a zigzag iridium chain with an elongation $d_z = 1.96 \text{ \AA}$. From left to right the panels show the bands for a paramagnetic calculation and for spin-orbit simulations, whereby the spins are oriented along the z , x , and y axes, respectively.

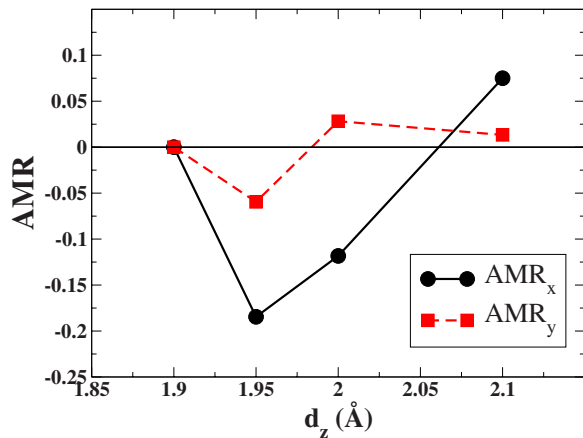


FIG. 6. (Color online) AMR ratios of iridium chains containing 21 atoms as a function of d_z .

We note that the spin-orbit interaction generates much larger gaps for iridium than for platinum. For this particular elongation, the gap when the spins point along the x axis is positioned exactly at the Fermi energy and has a value $E_g \approx 100$ meV at the Γ point. Using the estimated Fermi velocity $\hbar v_F \approx 1500$ meV d_z , we predict that chains containing about 15 atoms should show large magnetoresistance ratios.

To confirm this, we have simulated 2- and 21-atom-long iridium chains in contact to (111) iridium electrodes terminated by a pyramid, as in Fig. 1(a), for a number of elongations of the chain, which cover both the equilibrium distance

and also stretched situations. We have found that the magnetoresistive ratio of the two-atom chains was negligible for whatever elongation. In contrast, we have found that G_x is indeed substantially smaller than $G_{y,z}$ in the 21-atom chains. Our estimate of the AMR ratios, which we show in Fig. 6, therefore yields a negative AMR_x which can reach values as high as -0.2 . We stress that our previous analysis of Figs. 3 and 5 indeed led us to expect that AMR_x had to be of the order of -0.25 .

To summarize, we expect that short platinum chains should show a negligible magnetoresistance ratio until the number of atoms in the chain is of the order of 40. Since such long chains are very difficult to attain experimentally, we believe that platinum is not an optimum magnetoresistance material. We predict that a better candidate element is iridium. Shorter iridium chains are expected to display measurable magnetoresistance ratios. Longer chains could develop perfect magnetoresistance for certain elongations. These clear differences are experimentally accessible, and therefore we anticipate that future experimental studies of iridium chains will prove to be extremely fruitful.

We acknowledge useful conversations with C. Untiedt, J. J. Palacios, and A. Halbritter. L. Fernández-Seivane tested the gaps in platinum chains using the code QUANTUM ESPRESSO (<http://www.pwscf.org>). We acknowledge financial support from the European Union (Grant No. MRTN-CT-2003-504574), the Spanish MEC (Grant No. MEC-FIS2006-12117), and the UK EPSRC.

*ferrer@condmat.uniovi.es

¹P. Gambardella, A. Dallmeyer, K. Maiti, M. C. Malagoll, W. Eberhardt, K. Kern, and C. Carbone, *Nature (London)* **416**, 301 (2002).

²P. Gambardella, S. Rusponi, M. Veronese, S. S. Dhési, C. Grazioli, P. Dallmeyer, I. Cabria, R. Zeller, P. H. Dederichs, K. Kern, C. Carbone, and H. Brune, *Science* **300**, 1130 (2003).

³Y. Mokrousov, G. Bihlmayer, S. Heinze, and S. Blugel, *Phys. Rev. Lett.* **96**, 147201 (2006).

⁴L. Fernández-Seivane and J. Ferrer, *Phys. Rev. Lett.* **99**, 183401 (2007).

⁵T. O. Strandberg, C. M. Canali, and A. H. Macdonald, *Nature Mater.* **6**, 648 (2007).

⁶L. Fernández-Seivane, V. M. García-Suárez, and J. Ferrer, *Phys. Rev. B* **75**, 075415 (2007).

⁷A. Smogunov, A. dal Corso, R. Weht, A. Delin, and E. Tosatti, *Nat. Nanotechnol.* **3**, 22 (2008).

⁸H. Ohnishi, Y. Kondo, and K. Takayanagi, *Nature (London)* **395**, 780 (1998).

⁹A. I. Yanson, G. Rubio Bollinger, H. E. van den Brom, N. Agraït, and J. M. van Ruitenbeek, *Nature (London)* **395**, 783 (1998).

¹⁰R. H. M. Smit, Ph. D. thesis, Leiden University, 2003.

¹¹R. H. M. Smit, C. Untiedt, G. Rubio-Bollinger, R. C. Segers, and J. M. van Ruitenbeek, *Phys. Rev. Lett.* **91**, 076805 (2003).

¹²W. H. A. Thijssen, D. Marjensburgh, R. H. Bremmer, and J. M. van Ruitenbeek, *Phys. Rev. Lett.* **96**, 026806 (2006).

¹³H. Muramatsu, T. Hayashi, Y. A. Kim, D. Shimamoto, M. Endo, M. Terrones, and M. Dresselhaus, *Nano Lett.* **8**, 237 (2008).

¹⁴V. Rodrigues, J. Bettini, P. C. Silva, and D. Ugarte, *Phys. Rev. Lett.* **91**, 096801 (2003).

¹⁵A. Delin and E. Tosatti, *Phys. Rev. B* **68**, 144434 (2003).

¹⁶A. Delin, E. Tosatti, and R. Weht, *Phys. Rev. Lett.* **92**, 057201 (2004).

¹⁷W. Kohn and L. J. Sham, *Phys. Rev.* **140**, A1133 (1965).

¹⁸J. M. Soler, E. Artacho, J. D. Gale, A. García, J. Junquera, P. Ordejón, and D. Sánchez-Portal, *J. Phys.: Condens. Matter* **14**, 2745 (2002).

¹⁹L. Fernández-Seivane, M. A. Oliveira, S. Sanvito, and J. Ferrer, *J. Phys.: Condens. Matter* **18**, 7999 (2006).

²⁰The $\vec{L} \cdot \vec{S}$ term is nondiagonal in spin indices. As a consequence, a self-consistent implementation of the spin-orbit interaction requires a noncollinear implementation of density-functional theory.

²¹A. R. Rocha, V. M. García-Suárez, S. W. Bailey, C. J. Lambert, J. Ferrer, and S. Sanvito, *Phys. Rev. B* **73**, 085414 (2006).

²²V. M. García-Suárez, A. R. Rocha, S. W. Bailey, C. J. Lambert, S. Sanvito, and J. Ferrer, *Phys. Rev. Lett.* **95**, 256804 (2005).

²³J. P. Perdew and A. Zunger, *Phys. Rev. B* **23**, 5048 (1981).

²⁴N. Troullier and J. L. Martins, *Phys. Rev. B* **43**, 1993 (1991).

²⁵J. Fernández-Rossier, D. Jacob, C. Untiedt, and J. J. Palacios, *Phys. Rev. B* **72**, 224418 (2005).